Synthesis and Characterization of Fluorene-Based Low-Band Gap Copolymers Containing Propylenedioxythiophene and Benzothiadiazole Derivatives for Bulk Heterojunction Photovoltaic Cell Applications

JIN SU PARK,[1] TAE IN RYU,[1] MYUNGKWAN SONG,[1] KYUNG-JIN YOON,[1] MYUNG JIN LEE,[1] IN AE SHIN,[1] GI-DONG LEE,[2] JAE WOOK LEE,[3] YEONG-SOON GAL,[4] SUNG-HO JIN[1]

[1]Department of Chemistry Education and Interdisciplinary Program of Advanced Information and Display Materials, Pusan National University, Busan 609-735, Korea
[2]Department of Electronics Engineering, Dong-A University, Busan 604-714, Korea
[3]Department of Chemistry, Dong-A University, Busan 604-714, Korea
[4]Polymer Chemistry Lab., Kyungil University, Hayang 712-701, Korea

Received 1 November 2007; accepted 29 May 2008
DOI: 10.1002/pola.22928
Published online in Wiley InterScience (www.interscience.wiley.com).

ABSTRACT: The following noble series of soluble π-conjugated statistical copolymers was synthesized by palladium catalyzed Suzuki polymerization: poly[(9,9-dioctylfluorene)-*alt*-(4,7-bis(3′,3′-dihepyl-3,4-propylenedioxythienyl)-2,1,3-benzothiadiazole)] (PFO-PTBT) derived from poly(9,9-dioctylfluorene) (PFO) and poly[(4,7-bis(3′,3′-dihepyl-3,4-propylenedioxythienyl)-2,1,3-benzothiadiazole)] poly(heptyl$_4$-PTBT). The structure and properties of these polymers were characterized using ^{1}H-, ^{13}C-NMR, UV–visible spectroscopy, elemental analysis, GPC, DSC, TGA, photoluminescence (PL), and cyclic voltammetry (CV). The statistical copolymers, PFO-PTBT (9:1, 8.4:1.6, 6.5:3.5), were soluble in common organic solvents and easily spin coated onto indium-tin oxide (ITO) coated glass substrates. The weight-average molecular weight (M_w) and polydispersity of the PFO-PTBT ranged from (1.0–4.2) $\times$ 10^4 and 1.5–2.3, respectively. Bulk heterojunction photovoltaic cells with an ITO/PEDOT/PFO-PTBT:PCBM/LiF/Al configuration were fabricated, and the devices using PFOPTBT (6.5:3.5) showed the best performance compared with those using PFO-PTBT (9:1, 8.4:1.6). A maximum power conversion efficiency (PCE) of 0.50% (V_{oc} = 0.66 V, FF = 0.29) was achieved with PFO-PTBT (6.5:3.5). © 2008 Wiley Periodicals, Inc. J Polym Sci Part A: Polym Chem 46: 6175–6184, 2008
Keywords: conjugated polymers; fullerenes; copolymerization

INTRODUCTION

π-Conjugated polymers are expected to have great potential in future electronic and photonic devices, such as polymer light-emitting diodes (PLEDs),[1] organic photovoltaic cells (OPVs),[2] and organic thin film transistors (OTFTs).[3] The design of materials on the molecular level has the potential for efficient light emitting polymers covering the visible and near infrared spectrum. In addition, the harvesting of the entire solar spectrum by photovoltaic cells is an active research area. Polymer photovoltaic cells offer great technological potential as a renewable, alternative source for electrical energy. They can be flexible and be

Correspondence to: S. Jin (E-mail: shjin@pusan.ac.kr) and G.-D. Lee (E-mail: gdlee@donga.ac.kr)
Journal of Polymer Science: Part A: Polymer Chemistry, Vol. 46, 6175–6184 (2008)

made from solution cast processes such as spin coating, doctor blade, or screen-printing methods.[4] Among the different concepts that have been proposed in organic and/or polymer photovoltaic cells, the bulk heterojunction approach is attractive and has provided significant progress in improving the power conversion efficiency (PCE) of these devices in recent years. One of the possible ways of improving the PCE of photovoltaic cells is the implementation of new materials absorbing the part of the solar spectrum. Therefore, it is important to design and synthesize low-band gap polymers that improve the overlap of the polymer absorption spectrum with the standard solar spectrum under AM 1.5 global.[5,6] One successful approach for synthesizing low-band gap polymers is to arrange the electron-donor and electron-acceptor alternatively in repeating units along a polymer backbone.[7–9] From this synthetic design rule, a number of low-band gap polymers have been synthesized that reduces the band gaps to 0.3–0.5 eV compared with conventional π-conjugated polymers.[10] Polyfluorenes (PFs) containing two planarized benzene rings per monomeric unit have many advantages such as chemical and thermal stability, high photoluminescence (PL) quantum efficiency, and the ease of property tuning by copolymerization with various comonomers.[11] PFs are typical blue light-emitting polymers due to their wide-band gap. However, green and red light emitting fluorene-based copolymers can also be synthesized by incorporating low-band gap comonomers into the PF backbone.[12,13]

Poly(3,4-ethylenedioxythiophene) (PEDOT) has a variety of favorable properties, such as oxidation potential for conversion to a conducting state and high stability in conducting form with a low-band gap of 1.6 eV for use as a donor polymer in photovoltaic cells.[14] However, the poor solubility of PEDOT derivatives has been the biggest drawback for further applications in electrical and optical devices. A PEDOT derivative, poly (3′,3′-diheptyl-3,4-propylenedioxythiene) [poly (heptyl$_2$-PDOT)], was synthesized to solve this problem. This derivative provided good solubility behavior in organic solvents.[15] In addition, a novel low-band gap polymer, poly[4,7-bis(3′,3′-diheptyl-3,4-propylenedioxythienyl)-2,1,3-benzothiadiazole] [poly(heptyl$_4$-PTBT)] with electron-donating heptyl$_2$-PDOT segment and electron-withdrawing benzothiadiazole (BT) unit was synthesized to improve sunlight harvesting.[16]

This article reports the synthesis and characterization of a noble series of soluble π-conjugated statistical copolymers (PFO-PTBT) derived from poly(9,9-dioctylfluorene) (PFO) and poly[4,7-bis(3′,3′-dihepyl-3,4-propylenedioxythienyl)-2,1,3-benzothiadiazole] [poly(heptyl$_4$-PTBT)] by palladium catalyzed Suzuki polymerization.

EXPERIMENTAL

Materials and Characterization

All the reagents were purchased from Sigma-Aldrich and used without further purification. The solvents were purified using standard procedures and were handled in a moisture free atmosphere. Unless otherwise noted, these solvents were used without further purification. The ^{1}H- and ^{13}C-NMR spectra were recorded on a Bruker AM-300 spectrometer, and the chemical shifts were recorded in ppm units with chloroform as the internal standard. The UV–visible spectra were recorded with a Shimadzu UV-3100 spectrophotometer with a baseline correction, and normalization carried out using Microsoft Excel software. The emission spectra for the dilute solutions were determined using a Hitachi F-4500 fluorescence spectrophotometer. The solid state emission measurements were carried out by supporting each film on a quartz substrate, which was mounted to receive front-face excitation at an angle $< 45^\circ$. Each polymer film was excited with several portions of the visible spectrum using a xenon lamp. The molecular weight and polydispersity of the polymer were determined by gel permeation chromatography (GPC) using a PLgel 5 μm MIXED-C column on an Agilent 1100 series liquid chromatography system with THF as the eluent and calibration with polystyrene standards. Thermal analyses were carried out on a Mettler Toledo TGA/SDTA 851, DSC 822 analyzer under an N_2 atmosphere at a heating rate of 10 °C/min. Cyclic voltammetry (CV) was carried out in a 0.1 M solution of tetrabutylammonium tetrafluoroborate (Bu_4NBF_4) in anhydrous acetonitrile using a Bioanalytical Systems CV-50W voltammetric analyzer at a potential scan rate of 50–100 mV/s. Each polymer film was coated onto a Pt disc electrode (0.2 cm^2) by dipping the electrode into the polymer solution (10 mg/mL). A platinum wire was used as the counter electrode, and a Ag/$AgNO_3$ electrode was used as the reference electrode. All electrochemical experiments were performed at room temperature in a glove box in an Ar atmosphere.

Synthesis of 4,7-bis(3′,3′-diheptyl-2-bromo-3,4-propylenedioxythienyl)-2,1,3-benzothiadiazole (6)

4,7-Bis(3′,3′-diheptyl-3,4-propylenedioxythienyl)-2,1,3-benzothiadiazole (heptyl$_4$-PTBT) (5) (0.42 g, 0.50 mmol) was dissolved in DMF (10 mL) and *N*-bromosuccinimide (NBS) (0.18 g, 1.00 mmol) was added. The resulting mixture was stirred at room temperature in the dark for 12 h. After removing the DMF, the reaction mixture was extracted with chloroform and water. The organic layers were washed several times with water, dried over anhydrous $MgSO_4$, and filtered. The solvent was removed under reduced pressure and the mixture was purified by column chromatography in silica gel using chloroform/hexane (1:5) as an eluent to produce compound (6) as a dark red powder in 78% yield. ^{1}H-NMR ($CDCl_3$, δ ppm): 8.28 (s, 2H), 4.06 (s, 4H), 3.97 (s, 4H), 1.59–1.29 (m, 48H), 0.91 (m, 12H). ^{13}C-NMR ($CDCl_3$, δ ppm): 152.31, 147.94, 147.33, 147.20, 145.84, 127.44, 127.31, 123.64, 123.55, 123.48, 117.38, 114.15, 112.00, 96.19, 78.06, 44.12, 44.08, 32.12, 32.05, 30.61, 29.40, 23.04, 22.86, 14.31. HR-MASS: Calcd. For $C_{48}H_{70}Br_2N_2O_4S_3$: 992.2864, Found: 992.2873 [M^+].

Synthesis of Poly[{9,9-dioctylfluorene}-*co*-{4,7-bis(3′,3′-diheptyl-3,4-propylenedioxythienyl)-2,1,3-benzothiadiazole}] (PFO-PTBT) (5:5 mol %)

4,7-Bis(3′,3′-diheptyl-2-bromo-3,4-propylenedioxythienyl)-2,1,3-benzothiadiazole (6) (0.20 g, 0.20 mmol), 2,7-bis(4,4,5,5-tetramethyl-1,3,2-dioxaborolan-2-yl)fluorene (8) (0.13 g, 0.20 mmol), palladium(II) acetate (3.60 mg, 8.0 mol %) and tricyclohexylphosphine (4.5 mol %) were added to a dried three-neck flask in a nitrogen atmosphere. Dry toluene (2 mL) was added and the mixture was stirred at 90 °C for 5 min. An aqueous tetraethylammonium hydroxide solution (1.6 mL, 20% w/w) was then added and stirred for a further 24 h. During polymerization, a small amount of dry toluene was added to reduce the viscosity of the solution. 2-(Anthracen-9-yl)-4,4,5,5-tetramethyl-1,3,2-dioxaborolane (0.06 g, 0.20 mmol) was added to the mixture and stirred for 1 h. This was followed by the addition of 9-bromoacthracene (0.10 g, 0.40 mmol). After stirring for further 2 h, the mixture was cooled to room temperature and poured into stirring methanol (500 mL). The precipitate was dissolved in chloroform, and conc. NH_4OH was added and refluxed for 2 h at 70 °C to remove the residual catalyst and other impurities. After allowing the mixture to cool, the phases were separated, and the organic layer was washed several times with water. After pouring the chloroform solution into methanol (500 mL), the precipitated polymer was collected on a thimble filter and Soxhlet-extracted with methanol for 24 h followed by acetone and chloroform for 24 h in sequence. The polymer was precipitated into methanol, followed by filtration. The collected powder was dried under vacuum overnight at 40 °C to afford PFO-PTBT (5:5 mol %) (70 mg, 29%) as a dark purple powder. ^{1}H-NMR ($CDCl_3$, δ ppm): 8.42–8.23 (m, 2H), 7.66–7.90 (m, 6H), 4.2–4.0 (m, 8H), 2.08 (s, br, 4H), 1.57–1.27 (m, 80H), 0.73–0.93 (m, 18H). Anal calcd for S: 2.22. Found: 2.17.

Copolymers, poly[{9,9-dioctylfluorene}-*co*-{4,7-bis(3′,3′-diheptyl-3,4-propylenedioxythienyl)-2,1,3-benzothiadiazole}] (PFO-PTBT) with various feed ratios of 4,7-bis(3′,3′-diheptyl-2-bromo-3,4-propylenedioxythienyl)-2,1,3-benzothiadiazole (6) was synthesized using a similar method used to synthesize PFO-PTBT (5:5 mol %). PFO-PTBT (7:3 mol %) ^{1}H-NMR ($CDCl_3$, δ ppm): 8.42–8.23 (m, 2H), 7.66–7.90 (m, 6H), 4.2–4.0 (m, 8H), 2.08 (s, br, 4H), 1.57–1.27 (m, 80H), 0.73–0.93 (m, 18H). Anal calcd for S: 5.52. Found: 3.36. PFO-PTBT (9:1 mol %) ^{1}H-NMR ($CDCl_3$, δ ppm): 8.42–8.23 (m, 2H), 7.66–7.90 (m, 6H), 4.2–4.0 (m, 8H), 2.08 (s, br, 4H), 1.57–1.27 (m, 80H), 0.73–0.93 (m, 18H). Anal calcd for S: 7.86. Found: 6.20.

Fabrication of the Bulk Heterojunction Photovoltaic Cells

The bulk heterojunction photovoltaic cells were fabricated by spin-coating a 40 nm thick layer of PEDOT:PSS (Baytron P, Al 4083) on a ultrasonically cleaned 100 nm thick ITO coated patterned glass substrate. The coated substrates were then baked on a hot plate at 120 °C for 10 min. An active layer of the polymer was spin coated from a 1.5 wt % solution prepared in chlorobenzene after filtering through a 0.45-μm PP syringe filter. The ratios of the active layer as an electron donor and the methanofullerene [6,6]-phenyl C_{61}-butyric acid methyl ester (PCBM) as an electron acceptor was 1:4. The active layers (80 nm) were spin coated from chlorobenzene. The device structure was completed by depositing LiF (1 nm)/Al (150 nm) as the top electrode under a vacuum $< 3 \times 10^{-6}$ Torr in a vacuum evaporator attached to a glove box on the polymer active layer. The overlap of the two electrodes defined the active area of the photovoltaic cell, which was 4 mm^2. The

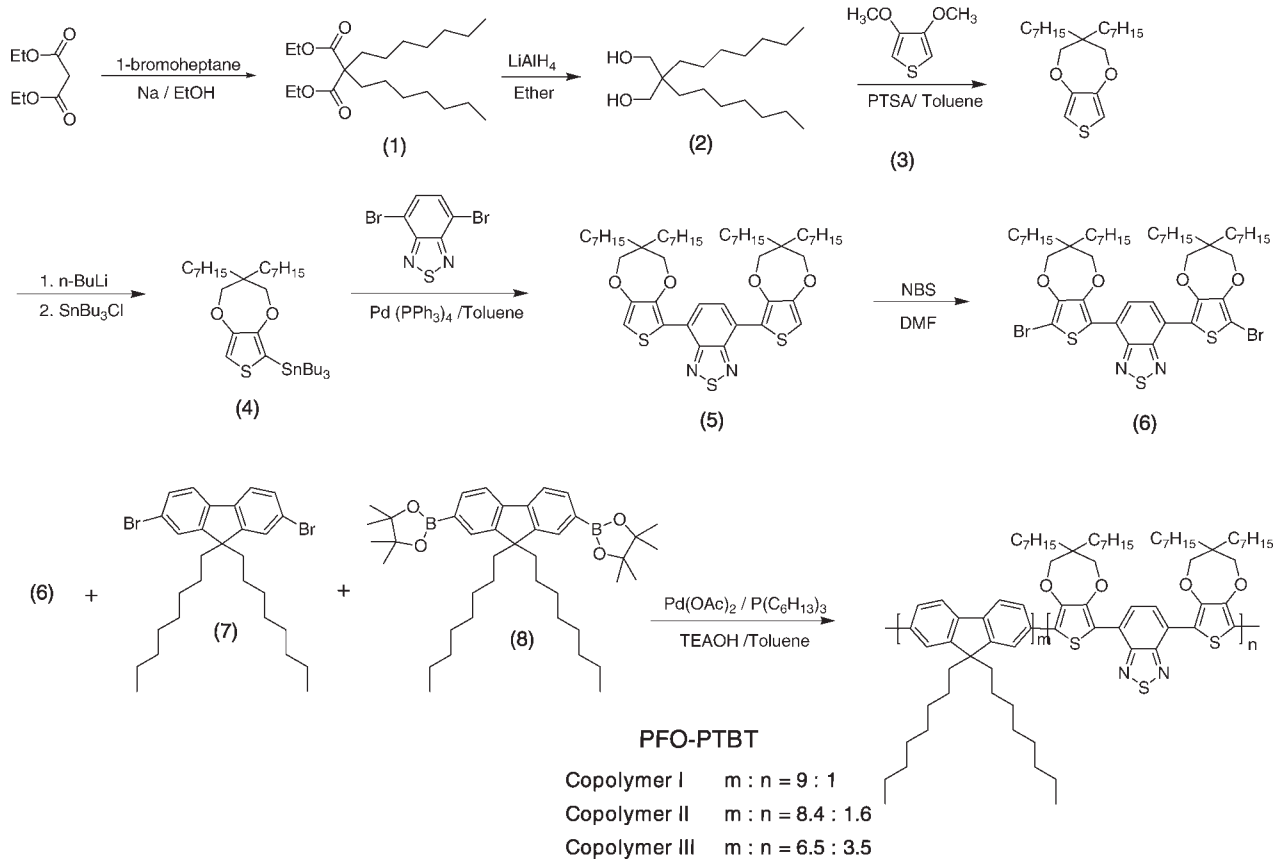

Scheme 1. Synthetic process of monomer and polymers.

performance of the photovoltaic cells was measured using a calibrated AM 1.5G solar simulator (Oriel 300 W) at a 100 mW/cm^2 light intensity adjusted with a standard PV reference cell (2 cm $\times$ 2 cm monocrystalline silicon solar cell, calibrated at NREL, Colorado, USA). The electric data was recorded using a Keithley 236 source-measure unit. All fabrication steps and characterization measurements were carried out in an ambient environment with out a protective atmosphere. The data was verified by fabricating each device at least five times.

RESULTS AND DISCUSSION

Scheme 1 outlines the synthetic routes of the monomer and the copolymers. 4,7-Bis(3′,3′-diheptyl-3,4-propylenedioxythienyl)-2,1,3-benzothiadiazole (heptyl$_4$-PTBT) (**5**), fluorene-based monomers **7** and **8** were synthesized using published procedures.[16,17] Compound **5** was dibrominated with NBS in DMF to afford compound **6** in 78% yield. In previous report, when BT unit was incorporated into PF backbone, the concentration of BT unit was even as low as 10% due to the poor solubility behavior of the resulting copolymer.[18] To solve this problem, we synthesized the novel low-band gap monomer **(6)** with the combination of two equivalent of electron-donating heptyl$_2$-PDOT and one equivalent of electron-withdrawing benzothiadiazole units. The low-band gap monomer **(6)**, 2,7-dibromo-9,9-dioctylfluorene **(7)**, and 9,9-dioctylfluorene-based diboronic ester **(8)** were copolymerized using the Suzuki cross-coupling method, as described by Chan et al.[19] and their characterization of photovoltaic properties of bulk heterojunction solar cells as an electron donor. The resulting statistical copolymers were precipitated in methanol, filtered, and redissolved in chloroform. The copolymer solutions were then washed with an aqueous ammonia solution to remove the residual catalyst using the previously reported procedures.[20] The monomer feed ratios were adjusted to examine the effects of various copolymer compositions on the UV–visible, PL,

Table 1. Polymerization Results and Thermal Properties of Copolymers

Polymer	M_w[a] ($\times 10^4$)	PDI[a]	Yield (%)	DSC[b] (°C)	TGA[c] (°C)
PFO-PTBT (6.5:3.5)[d]	1.0	1.5	41	105	373
PFO-PTBT (8.4:1.6)[d]	1.5	2.3	27	64	388
PFO-PTBT (9:1)[d]	4.2	1.9	31	65	403

[a] M_w and PDI of the polymers were determined by GPC using polystyrene standards.
[b] Determined by DSC at a heating rate of 10 °C/min under nitrogen.
[c] TGA was measured at temperature of 5% weight loss for the polymers.
[d] Composition ratio was determined from the sulfur content by elemental analysis.

and photovoltaic properties. The comonomer feed ratios of 9,9-dioctylfluorene to low-band gap monomer **(6)** were 9:1, 7:3, and 5:5 mol %, respectively. The composition ratios of the substituted fluorene to the low-band gap monomer in the copolymers were estimated from the sulfur content in the copolymers using elemental analysis. The PFO-PTBT (9:1) is in good agreement with the feed ratios of the two monomers within experimental error. However, PFO-PTBT (7:3) and PFO-PTBT (5:5) did not agree with the feeding ratio with larger fluorene monomer ratios than the feed ratio. The actual composition ratios of the two copolymers were PFO-PTBT (8.4:1.6) and PFO-PTBT (6.5:3.5), and the corresponding copolymers were named as PFO-PTBT (9:1), PFO-PTBT (8.4:1.6), and PFO-PTBT (6.5:3.5), respectively. This result might be due to the different reactivity of the two monomers **6** and **7** in addition to the relatively low-molecular-weight compared with the PFO-PTBT (9:1). The weight-average molecular weights (M_w) and polydispersity of the present copolymers were (1.0–4.2) $\times$ 10^4 and 1.5–2.3, respectively. Table 1 summarizes the polymerization results, molecular weights, and thermal data of the copolymers. By introducing the heptyl substituent into the 3,4-propylenedioxythiophene, the resulting low-band gap PF-based copolymers were completely soluble in common organic solvents such as chloroform, chlorobenzene, toluene, THF, and xylene. The chemical structures of the intermediates, monomers, and the copolymers were confirmed by ^{1}H-, ^{13}C-NMR spectroscopy, mass spectroscopy, and elemental analysis. The disappearance of the characteristic proton peaks of thiophene at 6.7 ppm in monomer **(6)** confirms the dibromination of compound **(5)**. All other peaks are in good agreement with the chemical structure of the materials. The ^{1}H-NMR spectra of the copolymers showed signals at $\sim$ 8.23–8.42 ppm and 7.66–7.90 ppm, which were assigned to the protons on the benzothiadiazole and the aromatic protons on the fluorene, respectively. The signals at 4.0–4.2 ppm were assigned to the methylene protons next to oxygen in the low-band gap segment, whereas 2.08 ppm was assigned to the protons on the octyl group substituted at the carbon-9 position of the fluorene ring. The intensity of signals at 4.0–4.2 ppm increased with increasing low-band gap segment ratio in the copolymers, while the signals at 2.08 ppm decreased. The thermal behavior of the copolymers was examined by DSC and TGA

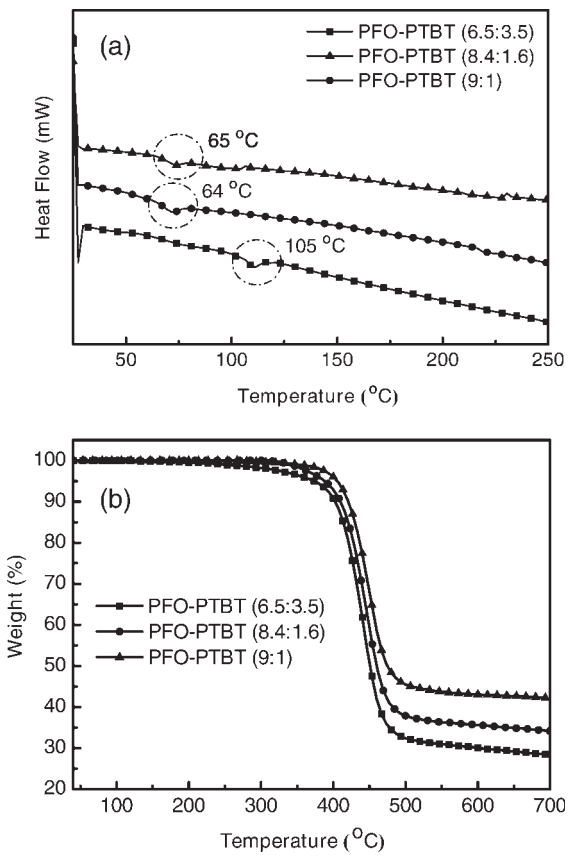

Figure 1. DSC (a) and TGA (b) thermograms of copolymers.

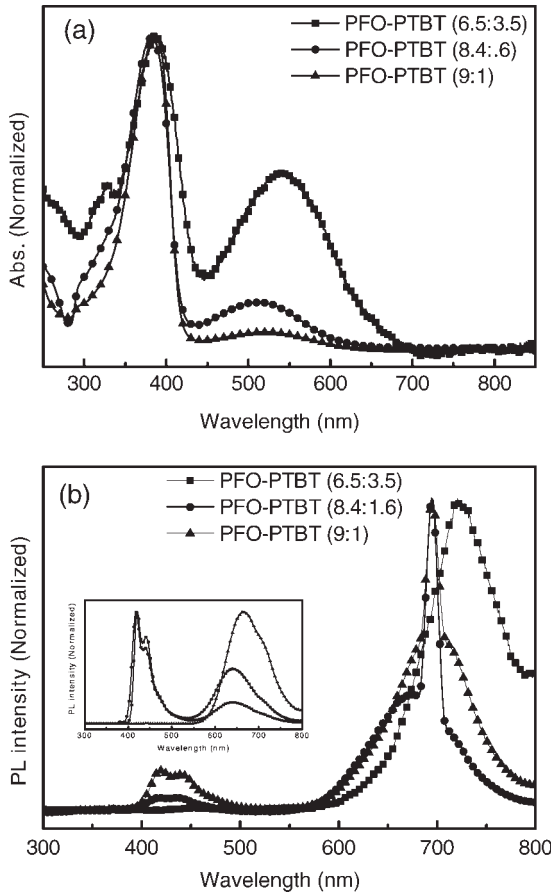

Figure 2. UV–visible absorption (a) and photoluminescence (PL) spectra (b) of the copolymers in film state. Inset: PL spectra of the copolymers in solution state.

thermograms, as shown in Figure 1. PFO-PTBT (8.4:1.6) and PFO-PTBT (9:1) exhibited a glass transition temperature (T_g) at $\sim$ 65 °C and PFO-PTBT (6.5:3.5) showed a higher T_g compared with the other ratios of copolymer. This is mainly due to the alternating copolymer nature of the PFO-PTBT (6.5:3.5) rather than to the random copolymer nature of PFO-PTBT (8.4:1.6) and PFO-PTBT (9:1). The thermograms of the copolymers showed 5% weight loss at 373–403 °C under a nitrogen atmosphere.

Figure 2(a) shows the normalized UV–visible absorption spectra of the copolymers in the thin films states. The absorption spectrum of the PFO-PTBT (6.5:3.5) has two broad peaks at 394 and 558 nm in the thin film state. The peak at 394 nm was assigned to the fluorene segment, and the peak at $\sim$ 558 nm was assigned to the absorption of the low-band gap segment. The absorption spectra of PFO-PTBT (8.4:1.6) and PFO-PTBT (9:1) showed similar peaks. Moreover, the absorption intensity at 558 nm increased gradually with increasing the content of the low-band gap segment in the polymer backbone. The optical band gaps calculated from the onset of the absorption of the PFO-PTBT (6.5:3.5), PFO-PTBT (8.4:1.6), and PFO-PTBT (9:1) were 1.73, 1.86, and 1.88 eV, respectively. Table 2 summarizes the maximum wavelengths of the absorption peak and the optical band gap of the copolymers.

Figure 2(b) shows the PL spectra of the copolymers in the thin film. PFO showed a PL peak at $\sim$ 420 nm in the film state.[21] In the solution state, compared with the PL spectrum of PFO-PTBT (6.5:3.5), the PFO-PTBT (8.4:1.6) and PFO-PTBT (9:1) showed two characteristic emission peaks, as shown in the inset of Figure 2(b). The one that appeared at 417 nm was attributed to emission from the PFO segments and the other peaks at 640–665 nm were assigned to the PTBT segments. Because of the low content of low-band gap segments in the copolymers, the PL spectra showed incomplete energy transfer from the wide-band gap of the PFO units to the low-band gap of the PTBT units. The PL spectra of the PFO-PTBT (8.4:1.6) and PFO-PTBT (9:1) have two maximum emission peaks at $\sim$ 420 nm and 696–772 nm in thin film corresponding to the PFO and PTBT

Table 2. Absorption, PL, and Energy Gap Data of Copolymers

	Abs_{max} (nm)		PL_{max} (nm)		
Polymer	Solution	Film	Solution	Film	E_g (eV)[a]
PFO-PTBT (6.5:3.5)	385, 540	394, 558	665	721	1.73
PFO-PTBT (8.4:1.6)	381, 509	381, 529	417, 439, 640	419, 441, 694[b]	1.86
PFO-PTBT (9:1)	388, 518	382, 545	421, 440, 636	418, 442, 695[b]	1.88

[a] Determined from the absorption edge of the UV–visible spectrum.
[b] Main peak in the UV–visible spectrum.

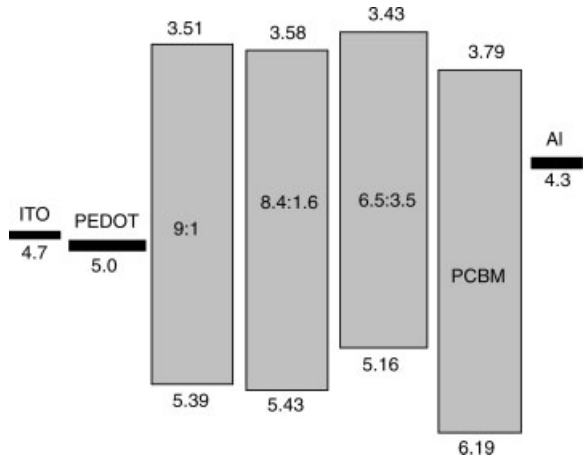

Figure 3. Energy band diagram of copolymers and PCBM.

segments, respectively. However, the intensity of the emission peaks at 420 nm was quietly quenched compared with the solution state. Therefore, there is much more energy transfer from PFO segments to the PTBT segments in PFO-PTBT (8.4:1.6) and PFO-PTBT (9:1) than in the solution state. PFO-PTBT (6.5:3.5) showed only one PL peak corresponding to the low-band gap segment in the solution and thin film states. This indicates more efficient energy transfer from the wide-band gap of PFO segments to the low-band gap of PTBT segments in PFO-PTBT (6.5:3.5). The PL peaks were slightly red-shifted with increasing content of low-band gap segments in the copolymers, from 696 nm for PFO-PTBT (9:1) to 772 nm for PFO-PTBT (6.5:3.5).

The electrochemical behavior of the copolymers was examined by cyclic voltammetry (CV) in a 0.1 M solution of tetrabutylammonium tetrafluoroborate (Bu_4NBF_4) in anhydrous acetonitrile. The highest occupied molecular orbital (HOMO) and lowest unoccupied molecular orbital (LUMO) levels of the copolymers with respect to the ferrocene/ferrocenium (4.8 eV) standard was calculated from the CV and band gap from the optical absorption spectrum.[22] Figure 3 shows the energy diagram of the copolymers and PCBM. The HOMO and LUMO energy levels decreased with increasing low-band gap of the PTBT segments to PFO-PTBT (6.5:3.5) compared with PFO-PTBT (9:1). From the decreased HOMO energy level of PFO-PTBT (6.5:3.5), a lower open-circuit voltage (V_{oc}) can be expected compared with that of PFO-PTBT (8.4:1.6) and PFO-PTBT (9:1).

Bulk heterojunction photovoltaic cells were fabricated using the copolymers as the electron donor and PCBM as the electron acceptor. The photovoltaic cell structure was ITO/PEDOT:PSS/PFO-PTBT:PCBM/LiF/Al using a 1:4 ratio of donor to acceptor materials at a fixed photoactive layer thickness of 80 nm. Table 3 lists the photovoltaic performance of these cells. The performance of these photovoltaic cells was examined by comparing the dark and illuminated current density-voltage (J-V) curves. The device fabricated with PFO-PTBT (6.5:3.5) showed a higher photovoltaic performance than the devices fabricated with PFO-PTBT (8.4:1.6) and PFO-PTBT (9:1) giving a J_{sc} of 1.55 mA/cm^2, a V_{oc} of 0.75 V, a FF of 0.31, and a PCE of 0.36%. On the basis of the UV–visible absorption spectra of the thin film, PFO-PTBT (6.5:3.5) possesses the best spectral coverage of visible light, and absorption coefficient of solar light from 400 to 700 nm is higher than the other copolymers. It was suggested that the upper limit to V_{oc} was found in the difference between the LUMO of the acceptor and the HOMO of the donor. However, the V_{oc} of the device with PFO-PTBT (6.5:3.5) was higher than that of the device with PFO-PTBT (8.4:1.6) and PFO-PTBT (9:1). To understand this phenomenon, AFM images of the

Table 3. Photovoltaic Properties of the Devices Made with Using Different Ratios of Copolymer to PCBM, (G)-PEDOT, and LiF/Al Cathode

Polymer	Buffer layer	V_{oc} (V)[a]	J_{sc} (mA/cm^2)[b]	FF[c]	PCE (%)[d]
PFO-PTBT (6.5:3.5)	PEDOT	0.75	1.55	0.31	0.36
	(G)-PEDOT	0.66	2.65	0.29	0.50
PFO-PTBT (8.4:1.6)	PEDOT	0.38	0.32	0.28	0.034
PFO-PTBT (9:1)	PEDOT	0.55	0.18	0.28	0.028

[a] V_{oc}: open-circuit voltage.
[b] J_{sc}: short-circuit current density.
[c] FF: fill factor.
[d] PCE: power conversion efficiency.

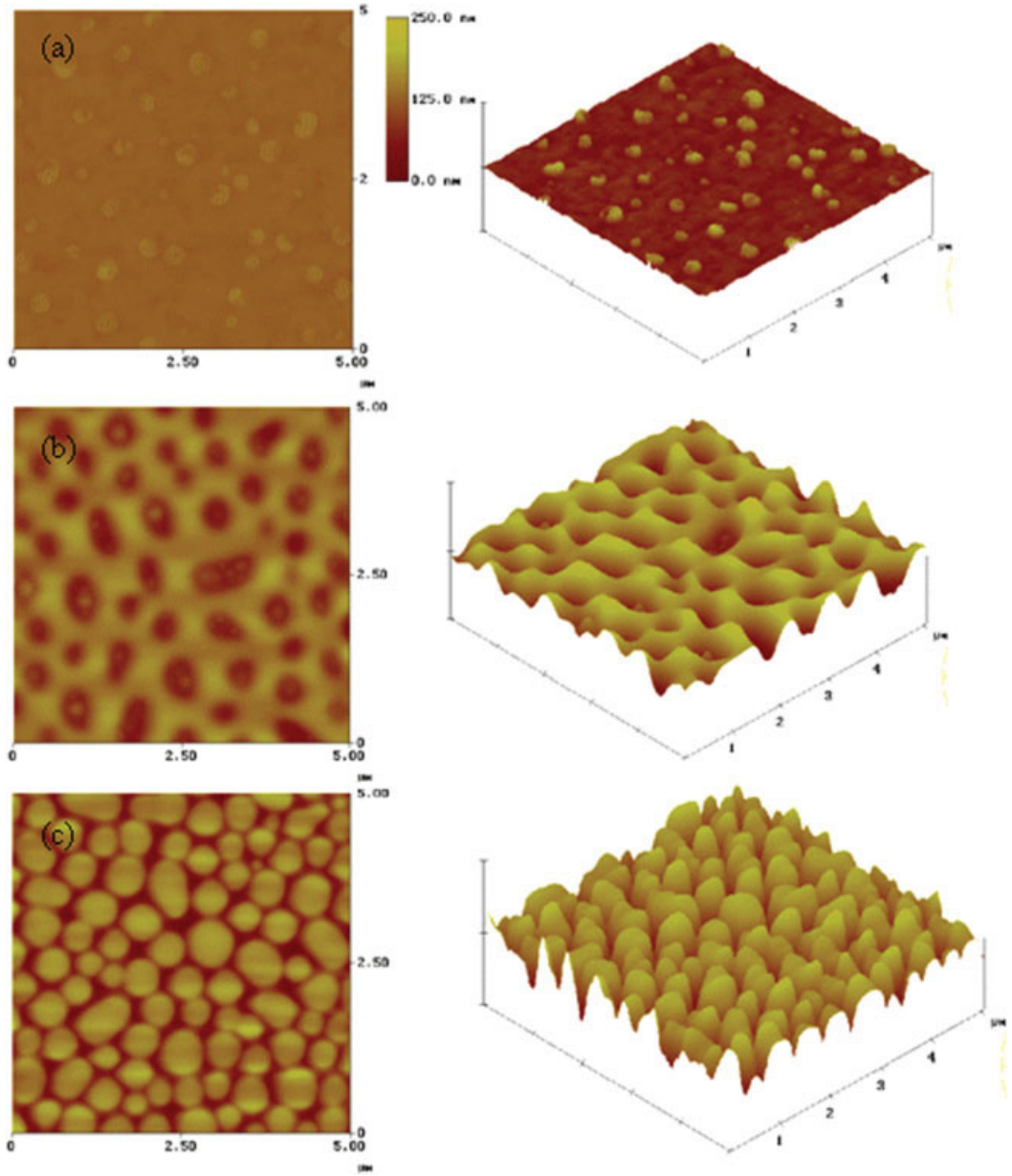

Figure 4. AFM topography images of copolymer:PCBM (1:4) spin-coated from chlorobenzene. (a) PFO-PTBT (6.5:3.5), (b) PFO-PTBT (8.4:1.6), and (c) PFO-PTBT (9:1).

copolymers were examined, as shown in Figure 4. The film morphology of PFO-PTBT (6.5:3.5) was relatively smooth with a r.m.s roughness of 14 nm compared with PFO-PTBT (8.4:1.6) and PFO-PTBT (9:1) with a r.m.s roughness of 43 and 52, respectively. Because of the high roughness in the PFO-PTBT (8.4:1.6) and PFO-PTBT (9:1), a partial leakage current might occur in the photovoltaic cells. The shunt resistance (R_{sh}) was smaller in the photovoltaic cells with PFO-PTBT (8.4:1.6) and PFO-PTBT (9:1), which decreased the V_{oc}.

It was shown that the addition of high molecular weight alcohol such as glycerol to PEDOT:PSS can increase its conductivity.[23] The conductivity of PEDOT:PSS increased from 1.26×10^{-2} S/cm to 1.51 S/cm for G-PEDOT:PSS by adding 6 wt % glycerol. Devices with G-PEDOT were fabricated using a 1:4 ratio of PFO-PTBT (6.5:3.5) and PCBM to determine the buffer layer effect on the

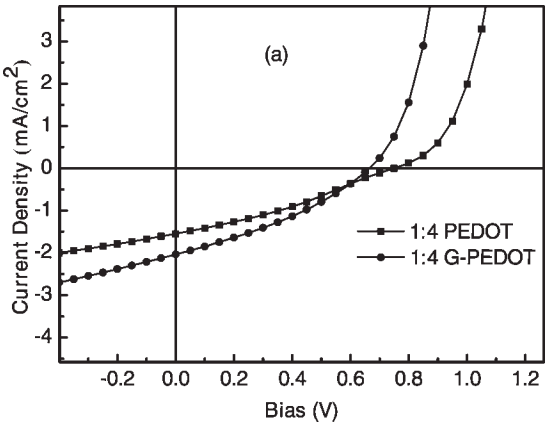

Figure 5. Current density-voltage (J-V) characteristics of the PFO-PTBT (6.5:3.5):PCBM blend of photovoltaic cells with PEDOT or G-PEDOT.

performance of bulk heterojunction photovoltaic cells. Figure 5 shows the measured J-V characteristics and Table 3 summarizes the results. With the 1:4 ratio of PFO-PTBT (6.5:3.5) to PCBM and G-PEDOT, the device showed a V_{oc}, J_{sc} and FF of 0.66 V, 2.65 mA/cm^2 and 0.29, respectively. From these values, the PCE was found to be 0.50%. An improved J_{sc} was observed for the G-PEDOT:PSS device due to the improved charge collection compared with the PEDOT:PSS device. This improvement might be due to the swelling and aggregation of the colloidal PEDOT-rich particles, forming a highly conducting network. Apart from this, the surface potential of the thin film will decrease due to the presence of glycerol in G-PEDOT. The increased J_{sc} improved the PCE of the device made from G-PEDOT:PSS to 0.36 and 0.50% for PFO-PTBT (6.5:3.5):PCBM (1:4) device, respectively. Studies aimed at optimizing the bulk heterojunction photovoltaic cells through thermal annealing as well as the donor to acceptor ratios for a better photovoltaic performance are currently underway.

CONCLUSIONS

A novel series of low-band gap polymers were synthesized for the more efficient harvesting of solar energy. An electron-deficient 2,1,3-benzothiadiazole units were introduced, and statistical copolymers, poly[(9,9-dioctylfluorene)-*alt*-(4,7-bis(3′, 3′-dihepyl-3,4-propylenedioxythienyl)-2,1,3-benzothiadiazole)] (PFO-PTBT) were synthesized in an attempt to achieve a lower-band gap. Bulk heterojuction photovoltaic cells with an ITO/(G-)PEDOT/PFO-PTBT:PCBM/LiF/Al were fabricated using PFO-PTBT as the electron donor and PCBM as the electron acceptor. The copolymer feed ratio was found to have a considerable effect on the PCE. The PCE of the copolymer photovoltaic cells increased with increasing PTBT content with a maximum PCE of 0.50% being achieved with PFO-PTBT (6.5:3.5).

This work was supported by the Korea Science and Engineering Foundation (KOSEF) grant funded by the Korea government (MOST) (No. M10600000157-06J0000-15,710).

REFERENCES AND NOTES

1. Burroughs, J. H.; Bradley, D. D. C.; Brown, A. R.; Marks, R. N.; Mackay, K.; Friend, R. H.; Burns, P. L.; Holmes, A. B. Nature 1990, 347, 539–541.
2. Brabec, C. J.; Sariciftci, N. S.; Hummelen, J. C. Adv Funct Mater 2001, 11, 15–26.
3. Yu, G.; Gao, J.; Hummelen, J. C.; Wudl, F.; Heeger, A. J. Science 1995, 270, 1789–1791.
4. Shaheen, S. E.; Radspinner, R.; Peyghambarian, N.; Jabbour, G. E. Appl Phys Lett 2001, 79, 2996–2998.
5. McCullough, R. D.; Lowe, R. D. J Chem Soc, Chem Commun 1992, 70–72.
6. Winder, C.; Sariciftci, N. S. J Mater Chem 2004, 14, 1077–1086.
7. Dhanabalan, A.; van Duren, J. K. J.; van Hal, P. A.; van Dongen, L. J.; Janssen, R. A. J. Adv Funct Mater 2001, 11, 255–262.
8. Roncali, J. Chem Rev 1997, 97, 173–206.
9. Jayakannan, M.; van Hal, P. A.; Janssen, R. A. J. J Polym Sci Part A: Polym Chem 2002, 40, 251–261.
10. Akoudad, S.; Roncali, J. Chem Commun 1998, 2081–2082.
11. Grell, M.; Bradley, D. D. C.; Inbasekaran, M.; Woo, E. P. Adv Mater 1997, 9, 798–802.
12. Cho, N. S.; Hwang, D. H.; Jung, B. J.; Lim, E.; Lee, J.; Shim, H. K. Macromolecules 2004, 37, 5265–5273.
13. Wang, F.; Luo, J.; Yang, V.; Chen, J.; Huang, F.; Cao, Y. Macromolecules 2005, 38, 2253–2260.
14. Sonmez, G.; Meng, H.; Wudl, F. Chem Mater 2004, 16, 574–580.
15. Shin, W. S.; Kim, M. K.; Jin, S. H.; Shim, Y. B.; Lee, J. K.; Lee, J. W.; Gal, Y. S. Mol Cryst Liq Cryst 2006, 444, 129–135.
16. Jin, S. H.; Kim, S. C.; Jung, S. J.; Kim, M. K.; Shin, W. S.; Lee, J. K.; Lee, J. W.; Gal, Y. S. J Polym Sci Part A: Polym Chem 2007, 45, 1394–1402.
17. Ranger, M.; Rondeau, D.; Leclerc, M. Macromolecules 1997, 30, 7686–7691.

18. Herguth, P.; Jiang, X.; Liu, M. S.; Jen, A. K. Y. Macromolecules 2002, 35, 6094–6100.
19. Chan, K. L.; Mckiernan, M. J.; Towns, C. R.; Holmes, A. B. J Am Chem Soc 2005, 127, 21, 7662–7663.
20. Svensson, M.; Zhang, F.; Veenstra, S. C.; Verhees, W. J. H.; Humelen, J. C.; Kwoon, J. M.; Inganäs, O.; Andersson, M. R. Adv Mater 2003, 15, 12, 988–998.
21. Yang, R.; Tian, R.; Yan, J.; Zhang, Y.; Yang, J.; Hou, Q.; Yang, W.; Zhang, C.; Cao, Y. Macromolecules 2005, 38, 244–253.
22. Jandke, M.; Strohriegl, P.; Berleb, S.; Werner, E.; Brutting, W. Macromolecules 1998, 31, 6434–6443.
23. Kim, W. H.; Mäkinen, A. J.; Nikolov, N.; Shashidhar, R.; Kim, H.; Kafafi, Z. H. Appl Phys Lett 2002, 80, 3844–3846.